THE JOURNAL OF BIOLOGICAL CHEMISTRY
Vol. 271, No. 18, Issue of May 3, pp. 10640–10647, 1996

Printed in U.S.A.

The Conformational Properties of the Highly Selective Cannabinoid Receptor Ligand CP-55,940*

(Received for publication, October 16, 1995, and in revised form, February 12, 1996)

Xiang-Qun Xie‡§, Lawrence S. Melvin¶, and Alexandros Makriyannis‡§‖**

From the ‡Institute of Materials Science and the ‖Department of Pharmaceutical Sciences, School of Pharmacy, The University of Connecticut, Storrs, Connecticut 06269, the §Francis Bitter National Magnet Laboratory, Massachusetts Institute of Technology, Cambridge, Massachusetts 02139, and the ¶Central Research, Pfizer Inc., Groton, Connecticut 06340

During a search for novel drugs possessing analgesic properties but devoid of the psychotropic effects of marijuana, a group of molecules designated as nonclassical cannabinoids was synthesized by Pfizer. Of these nonclassical cannabinoids CP-55,940 has received the most attention principally because it was used as the high affinity radioligand during the discovery and characterization of the G-protein-coupled cannabinoid receptor. In an effort to obtain information on the stereoelectronic requirements at the cannabinoid receptor active site, we have studied the conformational properties of CP-55,940 using a combination of solution NMR and computer modeling methods. Our data show that for the most energetically favored conformation, (i) the aromatic phenol ring is perpendicular to the cyclohexane ring, and the phenolic O–H bond is coplanar with the aromatic ring and points away from the cyclohexyl ring; ii) the dimethylheptyl chain adopts one of four preferred conformations in all of which the chain is almost perpendicular to the phenol ring; and iii) an intramolecular H-bond between the phenolic and hydroxypropyl groups allows all three hydroxyl groups of CP-55,940 to be oriented toward the upper face of the molecule. Such an orientation by the OH groups may be a characteristic requirement for cannabimimetic activity.

The psychoactive effects of cannabinoids, particularly Δ^9-tetrahydrocannabinol (Δ^9-THC),[1] are well documented and offer a vexing target for new therapeutic drug discovery. Potential therapeutic applications include analgesia, sedation, attenuation of the nausea and vomiting due to cancer chemotherapy, appetite stimulation, decreasing intraocular pressure in glaucoma, certain motor or convulsant disorders, and concentration-time deficits (1, 2). A most probable site at which many of the pharmacological effects of cannabimimetics are induced is now thought to be the cannabinoid receptor (CB). This receptor type (CB1 and CB2 subtypes are described) is a subgroup of the G_i-protein-coupled seven transmembrane spanning receptor superfamily (3). The CB1 receptor subtype is found predominately in brain (4, 5), whereas the CB2 receptor subtype is reported only in peripheral tissue (6).

A series of compounds was designed, synthesized, and designated as nonclassical cannabinoids (NCCs), *e.g.* CP-55,940 in Fig. 1, which differ from classical cannabinoids by the absence of a tetrahydropyran ring, *e.g.* Δ^9-THC and (−)9β-OH-hexahydrocannabinol (7, 8). Although the NCCs possess significant analgesic activity, there was sufficient data to indicate that these NCC molecules still exhibit the behavioral effects of the classical analogs (9, 10). Key pharmacophores for the NCC analogs include a phenolic hydroxyl (Ph-OH), an aliphatic side chain attached to the phenyl ring, and a cyclohexyl ring (C-ring), all of which are also present in the natural cannabinoid Δ^9-THC. Two additional pharmacophores, the northern and southern aliphatic hydroxyl groups, are not found in the natural cannabinoids but are present in most NCCs. The presence of these aliphatic hydroxyl groups significantly enhances the analgesic activity in the NCC series (8). Consequently, the spatial arrangement with regard to the molecular pharmacophores should play an important role in determining CB1 receptor binding affinity and pharmacological activity.

The conformational properties of the NCCs still remained to be investigated in detail. Of the nonclassical analogs, one particularly potent and enantioselective derivative, CP-55,940, has received extensive attention because it was used as a radiolabel for the identification and characterization of the cannabinoid receptor (11). CP-55,940 is structurally similar to its prototype, CP-47,497, except for having a hydroxypropyl group (southern aliphatic OH) on the C-ring. This structural modification incorporated in CP-55,940 enhances CB1 receptor binding potency by 20-fold and enantioselectivity for CB1 receptor binding by 44-fold (12). As an analgesic, it is 10 times more potent than CP-47,497 and about 100 times more potent than Δ^9-THC (8, 10). In an earlier publication (7, 13), we reported preliminary results on the conformational properties of prototype CP-47,497.

In this report, we examine the conformational properties of CP-55,940 in order to define within this important ligand those stereoelectronic features most probably associated with cannabimimetic activity and receptor binding. To accomplish our goal, we have combined two-dimensional high resolution NMR and computer modeling techniques to study the conformational properties of CP-55,940 while paying special attention to: (i) the relative orientation of the C-ring with respect to the A-ring; (ii) the conformation of the phenolic Ph-OH group; and (iii) the conformation of the 1,1-dimethylheptyl side chain.

EXPERIMENTAL PROCEDURES

Materials—CP-55,940 was a generous gift from Pfizer Central Research (Groton, CT). NMR samples were prepared in $CDCl_3$ (99.8 atom

* This project was supported by Grants DA-3801, DA-07215, and DA-00152 from the National Institute on Drug Abuse. The costs of publication of this article were defrayed in part by the payment of page charges. This article must therefore be hereby marked "*advertisement*" in accordance with 18 U.S.C. Section 1734 solely to indicate this fact.

** To whom correspondence should be addressed: Dept. of Pharmaceutical Sciences, U-92, School of Pharmacy, University of Connecticut, Storrs, CT 06269. Tel.: 860-486-2133; Fax: 860-486-3089.

[1] The abbreviations used are: Δ^9-THC, (−)-Δ^9-tetrahydrocannabinol; NCC, nonclassical cannabinoids; Ph-OH, phenolic hydroxyl; C-ring, cyclohexyl ring; A-ring, phenol ring; COSY, correlation spectroscopy; DQF, double quantum filter; NOESYPH, phase-sensitive ^{1}H-^{1}H nuclear Overhauser enhancement spectroscopy; HMQC, heteronuclear multiquantum coherence; DMH, 1,1-dimethylheptyl; NOE, nuclear Overhauser effect; H-bond, hydrogen bond.

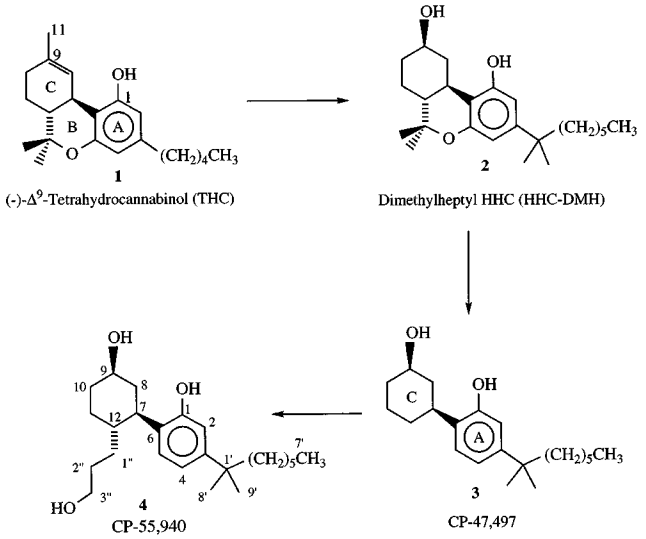

FIG. 1. **Evolution in cannabinoid structures with progressively enhanced potencies from the naturally occurring Δ^9-THC toward the potent synthetic analogs.**

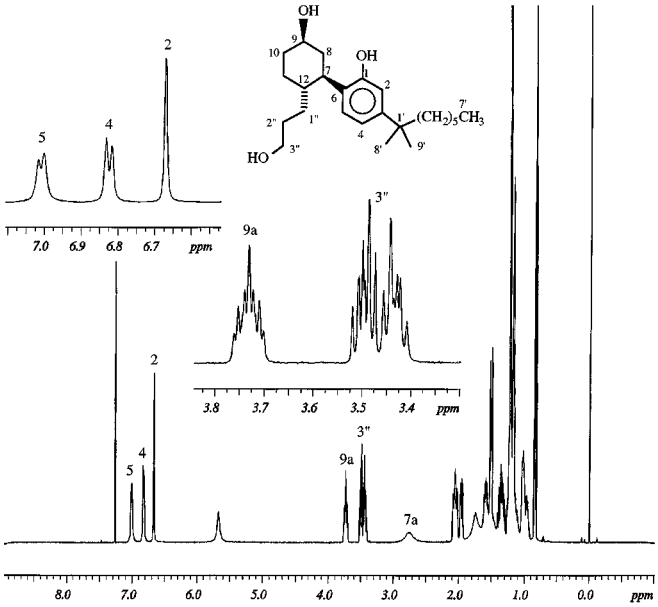

FIG. 2. **500 MHz ^{1}H spectrum of CP-55,940 in $CDCl_3$ at 298 K in full and expanded scales.**

%) at concentrations of 0.02 M for ^{1}H and 0.2 M for ^{13}C, filtered, degassed, and sealed in 5 mm NMR tubes. Tetramethylsilane was used as an internal chemical shift reference.

NMR Spectra—The high resolution one- and two-dimensional NMR spectra were obtained on Bruker AMX-500 and WP-200SY spectrometers. One-dimensional ^{1}H 500 MHz NMR spectra were recorded using the acquisition parameters: pulse width, 5.0 μs; spectral width, 4990.0 Hz; data size, 16 k; recycling delay, 2 s; number of transients, 16; temperature, 298 K. Two-dimensional phase-sensitive ^{1}H-^{1}H chemical shift correlation spectra with double quantum filter (DQF-COSY) (14) were obtained at 500 MHz with the acquisition parameters: 90 ° pulse width, 5 μs; spectral width, 4990.0 Hz; recycling delay, 1.3 s. The data were 512 w in the F1 dimension and 2k in the F2 dimension and were zero-filled in F1 prior to two-dimensional Fourier transformation to yield a 2k × 2k data matrix. The spectra were processed using a shift sine-bell window function in both dimensions. Two-dimensional phase-sensitive ^{1}H-^{1}H nuclear Overhauser enhancement spectra (NOESYPH) (15) were collected at 500 MHz using the acquisition parameters similar to the DQF-COSY with the addition of mixing time (800 ms). Two-dimensional chemical exchange spectra were performed using the same pulse sequence as in NOESYPH (16) to assign the obscured aliphatic OH resonance. In the spectrum, the positive cross-peaks were observed due to the exchange among the hydroxyl groups. Two-dimensional ^{1}H-^{13}C inverse correlated experiments with heteronuclear multiquantum coherence (HMQC) (17) were performed at 500 MHz (for ^{1}H) using the inverse detection probe with the acquisition parameters: 90 ° and 180 ° pulses for ^{1}H, 8.4 and 16.8 μs, and for ^{13}C, 12.2 and 24.4 μs; decoupling high power, 2 dB; decoupling low power, 18 dB; J_{C-H} value delay time, 3.57 ms; delay for bilinear rotation decoupling inversion pulse, 0.35 s; increment, 9 μs; number of scans, 8; for ^{1}H, SI2 = 1024k, TD2 = 512w, SW = 4716.98 Hz; for ^{13}C, SI1 = 4096k, TD1 = 1024k, SW = 220.85 ppm. Simulations of one-dimensional ^{1}H NMR spectra were performed with Bruker's LAOCOON-based PANIC software (18) using procedures that we have described elsewhere (13, 19).

Computer Molecular Modeling—Molecular modeling and graphic display were performed on an 4D/70GT IRIS Silicon Graphics workstation using the Biosym InsightII/Discover molecular modeling package (21). The structure of CP-55,940 was built from the molecular model of Δ^9-THC, which was initially generated from the x-ray crystallographic data of Δ^9-tetrahydrocannabinolic acid (22) and energy-minimized using the Biosym program. The minimum energy conformation of Δ^9-THC was then used as a starting template on which the structures of CP-55,940 were generated by deletion and/or addition of atoms at standard bond lengths and bond angles under the Biosym software.

Molecular mechanics/dynamics calculations (13, 23) were carried out using a Biosym-interfaced AMBER force field (24, 34) with the following three steps: 1) initial structure was minimized to relieve any overly strained coordinates; 2) molecular dynamics sampling was performed using the following protocol with time steps of 1 fs: (i) heat up to 2500 K and equilibrate for 1 ps and (ii) dynamics simulation at this temperature for 300 ps with atomic coordinate trajectories recorded every 1 ps; and 3) the 300 frames recorded during the dynamics run were retrieved and minimized with a two-step minimization, using the steepest descent method for the first 100 iterations and then the conjugate gradient method until the maximum derivative was less than 0.001 kcal/mol. The calculations were carried out in a vacuum condition (default, dielectric constant = 1). A total of 300,000 conformations or frames were sampled during the simulation. In order to reduce the volume of the output data to a more manageable level, conformer structures were recorded at 1-ps intervals, thus reducing the number of structures to be analyzed to 300 frames. For a molecule like CP-55,940 with several flexible substituents other than the hydroxypropyl chain, the dynamics calculations would have to sample too many conformations. Therefore, we imposed restraints on the torsional angles of certain regions, such as the DMH chain (except for the two dihedral angles adjacent to the A-ring, φ_3 and φ_4, in Table III), the C-ring, and the Ph-OH, which we found to be similar to that of its earlier studied congener CP-47,497. To avoid a formation of *cis* or *gauche* segments in the DMH side chain and to evade possible *chair-boat* interconversions in the cyclohexyl ring, a torsional restraint of 100 kcal/rad^2 was added to the corresponding torsion angles in those regions. This effectively eliminated unnecessary *trans-cis* or *chair-boat* conversions. A torsional force was also applied into our dynamics strategy to restrict the orientation of the phenolic OH on the basis of the NOE data in which the Ph-OH proton faces the adjacent aromatic H-2 proton. Such an external torque about the specific dihedral angles tends to force the calculation toward certain restrictions during dynamics sampling, thus biasing the molecule to the region of interest. Dihedral drive techniques (13) were performed to calculate rotational energy barriers with intervals of 5 ° for one-bond rotation and 10 ° for two-bond rotation. Finally, an additional torsion force (200 kcal/rad^2) was applied to restrain the rotated dihedral angle when applying energy minimization to relax the whole molecule.

RESULTS

NMR Spectral Assignments—The spectral assignments of CP-55,940 were initially made by analogy with the chemical shifts of CP-47,497 reported elsewhere (13) and then specifically assigned on the basis of the coupling connectivities in the ^{1}H-^{1}H COSY spectrum and confirmed by the ^{1}H-^{13}C HMQC spectrum. The full and expanded scales of one-dimensional NMR spectrum are shown in Fig. 2. The assignments of the cyclohexyl protons were achieved on the basis of integrated chemical shifts and analysis of the expanded regional contour plot of the DQF-COSY spectra. A logical starting point is the resonance of H-9a at δ 3.74 ppm, which shows vicinal coupling to H-10e, H-8e, H-10a, and H-8a. We could assign the proton signals of H-10e and H-10a at δ 2.09 ppm and δ 1.38 ppm with the support of the cross-peak connectivities of H-9a with H-10a,

H-8a, H-10e, and H-8e. The COSY spectrum (Fig. 3) clearly shows three components (H-10e, H-8e, and H-11e) under the multiplet at 2.06 ppm, in which three related strong geminal ^2J couplings, H-10e/a (F1 = 2.09, F2 = 1.38 ppm), H-8e/a (F1 = 2.05, F2 = 1.53 ppm), and H-11e/a (F1 = 1.98, F2 = 1.13 ppm) can be discerned. In order to confirm the assignments made above, two-dimensional heteronuclear ^{1}H-^{13}C correlated experiments were performed to gain information about the H-C connectivities. Fig. 4 shows the two-dimensional ^{1}H-^{13}C HMQC spectra with enhancement of ^{13}C sensitivity. The cross-peaks serve to identify the H-C connectivities. The complete assignments of proton and carbon chemical shifts for CP-55,940 are summarized in Table I. While comparing the above assignments with those of CP-47,497 (13), we found that most of the proton resonances of CP-55,940 are very similar to the corresponding ones of CP-47,497. Variations, however, could be seen in the proton chemical shifts of the cyclohexyl ring of CP-55,940 due to the presence of the hydroxypropyl side chain. Our two-dimensional ^{1}H-^{1}H COSY spectrum (Fig. 3) also showed that each of the 2″-CH_2 methylene protons had cross-peaks with the 3″-CH_2 methylene protons. The separation of the two cross-peaks is about 0.28 ppm, indicating that the two protons of 2″-CH_2 are nonequivalent (see "Discussion").

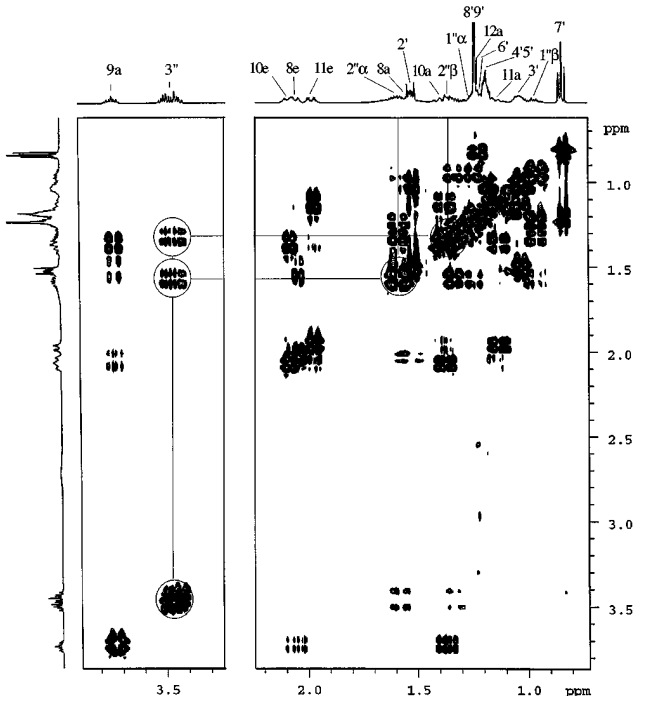

FIG. 3. **Expanded scale of a 500 MHz two-dimensional COSY-PH-DQF spectrum of CP-55,940 in $CDCl_3$ solution at 298 K.**

Coupling Constant Measurements—Coupling constants were measured and refined using a method described elsewhere (13). ^2J and ^3J values were first approximated from the two-dimensional DQF-COSY spectra, which offered a better resolution of cross-peaks (25). The chemical shift values (Table I) and approximated J values were then used as the starting point for an iterative simulation of the subspectra thus allowing us to refine ^2J and ^3J values (Table II). ^3J values so obtained were then incorporated into the Karplus equation (18) as we have described elsewhere (13, 19) to calculate the corresponding dihedral angles (Table II), which indicated a typical chair conformation of the C-ring.

NOE Interactions—NOE is one of the most important NMR parameters used in conformational analysis because the magnitude of the NOE is inversely proportional to the sixth power of the interproton distance in space ($I_{NOE} \propto r^{-6}$). Typically, an observed NOE cross-peak indicates that the two protons are near in space within a distance of 3.0 Å and exhibit through space coupling with each other. Beyond the 3.0 Å range, the

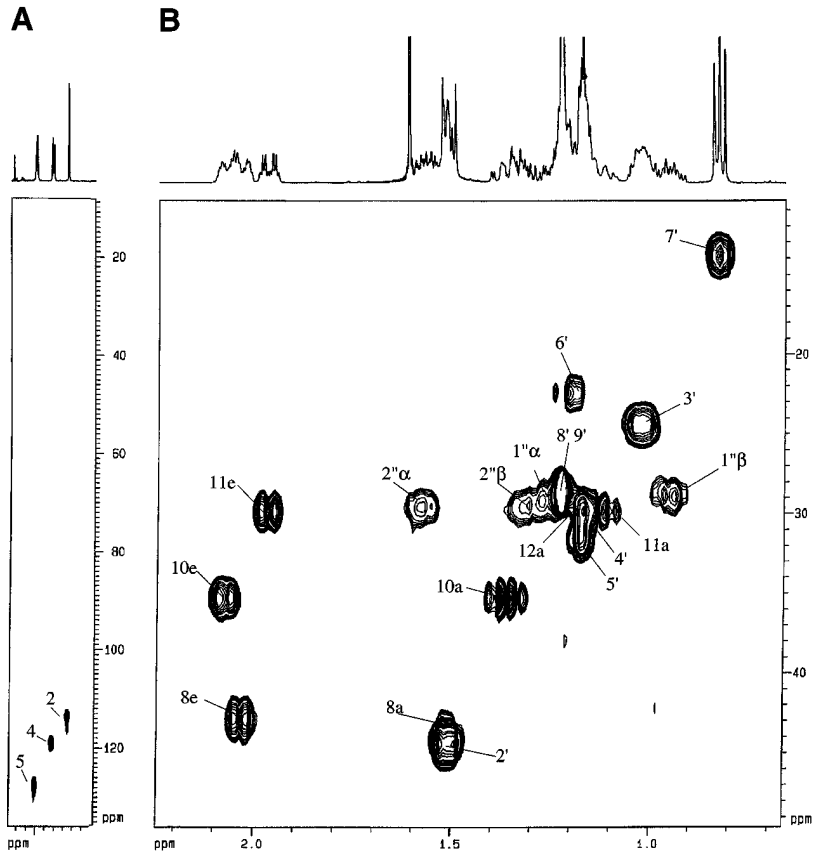

FIG. 4. **500 MHz two-dimensional ^{1}H-^{13}C inverse correlation spectrum (HMQC) of CP-55,940 in $CDCl_3$ at 300 K (^{13}C one-dimensional external spectrum is not displayed at F1 dimension).** *A*, the downfield region showing the aromatic resonances. *B*, the expanded scale of the upfield region showing ^{1}H-^{13}C coupling for the aliphatic resonances.

TABLE I
^1H NMR at 500 MHz and ^{13}C NMR at 125 MHz chemical shift assignments for CP-55,940 in $CDCl_3$ solution at 298 K and 300 K, respectively

Hydrogen	Chemical shift	Carbon	Chemical shift
	ppm		*ppm*
2	6.68	1	152.73
4	6.84	2	113.65
5	7.02	3	149.01
7	2.72	4	118.99
8e	2.05	5	127.52
8a	1.53	6	127.70
9a	3.75	7	39.30
10e	2.09	8	44.17
10a	1.38	9	71.18
11e	1.98	10	35.53
11a	1.13	11	30.03
12a	1.26	12	29.45
2′	1.53	1′	37.28
3′	1.03	2′	44.73
4′	1.18	3′	24.65
5′	1.19	4′	30.06
6′	1.22	5′	31.81
7′	0.84	6′	22.69
8′,9′	1.23	7′	14.11
1-OH	5.08	8′,9′	28.91
9-OH	1.55		
3″-OH	1.24		
1″	0.98, 1.25	1″	29.08
2″	1.31, 1.59	2″	29.70
3″	3.45, 3.50	3″	63.38

TABLE II
^1H NMR coupling constants and calculated dihedral angles for CP-55,940

Type of coupling	H′:H	Coupling constant ^nJ value[a]	Dihedral angle[b]
		Hz	*degrees*
Geminal ^2J	8a-8e	−12.5	[c]
	10a-10e	−12.6	[c]
	11a-11e	−12.5	[c]
	2″ab	−10.0	[c]
	3″ab	−10.4	[c]
Vicinal ^3J	7a-8a	10.5	156
	7a-8e	4.0	58
	7a-12a	12.5	180
	8a-9a	10.8	158
	8e-9a	4.3	57
	9a-10a	10.8	158
	9a-10e	4.3	57
	10a-11a	11.7	161
	10a-11e	4.1	57
	10e-11a	4.0	58
	10e-11e	2.2	65
	3″a-2″a	6.6	[d]
	3″a-2″b	6.7	[d]
	3″b-2″a	6.0	[d]
	3″b-2″b	6.3	[d]

[a] Determined from one- or two-dimensional spectra and refined through spectral simulation using PANIC. n is the number of bonds through which coupling occurs (geminal, $n = 2$, vicinal, $n = 3$).
[b] Calculated using the equation $^3J = K\cos^2\phi$; where $K_{a\text{-}a} = 12.5$ Hz, $K_{a\text{-}e} = K_{e\text{-}a} = 14.3$ Hz, and $K_{e\text{-}e} = 12.9$. ϕ is the dihedral angle. K values are calculated from 1,3,5-trimethyl-cyclohexane (19, 20).
[c] Geminal bond angles cannot be quantitatively determined.
[d] This vicinal bond angle cannot be quantitatively determined. Computer simulations show slightly nonequivalent coupling constants for the protons of 2″-CH_2 and 3″-CH_2. Individual methylene protons are separated by 0.28 ppm for 2″-CH_2: H-2″a (1.59 ppm) and H-2″b (1.31 ppm); by 0.05 ppm for H-3″; H-3″a (3.45 ppm) and H-3″b (3.50 ppm).

NOE is very weak, and the effect becomes barely detectable at 4.5 Å (26). To obtain the NOE values for the protons of CP-55,940, the two-dimensional ^1H-^1H phase-sensitive NOESY spectrum was obtained (Fig. 5). Our data show an NOE cross-peak between the phenol hydroxyl proton (δ 5.28 ppm) and the adjacent aromatic H-2 proton (δ 6.68 ppm), indicating that these two protons are spatially near and coupled through a dipole-dipole interaction. As will be discussed later, this result is used to assign the orientation of the phenolic OH proton. Another two NOE cross-peaks were identified as being due to spatial coupling between H-5 with H-8a and H-12a, indicating that H-5 is near H-8a and H-12a. Such cross-peaks provide important information regarding the preferred orientation of the A-ring with respect to the C-ring as shown in Fig. 5. The NOE cross-peak pattern that was observed between the DMH side chain and the aromatic ring protons (Fig. 5) indicates that the conformation of the DMH chain of CP-55,940 is very similar to one observed for CP-47,497, in which the DMH side chain is almost perpendicular to the plane of phenolic ring (13).

Computational Results—Molecular dynamics/mechanics was used to search for the preferred conformations of CP-55,940 and to examine the possibility of intramolecular H-bonding between hydroxyl groups. The main advantage of using molecular dynamics is that it simulates molecular motion at high temperature, thus increasing the probability of inducing conformational transitions past any possible high energy barriers. This would ensure sampling of all possible minima while avoiding the risk of a situation in which the molecular mechanics calculation might lead to a local rather than the global energy minimum. Dynamics simulations were performed with time steps of 1 fs for 300 ps. The data were recorded at 1-ps intervals, and a total of 300 frames of conformers were sampled. Molecular mechanics energy minimizations were carried out for each of the 300 conformers while releasing all torsional angle constraints. This operation resulted in a convergence of these conformers into several families. Of these families, the six energetically lowest are shown in Fig. 6. Conformers II, III, IV, V, and VI allow for intramolecular H-bonding between the hydroxypropyl and the phenolic hydroxyl groups if we assume that hydroxyl groups separated by approximately 2 Å will form a H-bond. Such H-bonding imparts greater stability to each of the five conformers. The most stable of these is conformer IV, which is also the global energy minimum. Conformer II, with the Ph-OH/3″-OH hydrogen bond on the opposite face of the molecule, has only 0.28 kcal/mol higher energy than that of conformer IV. The summary of the calculated structural features of CP-55,940 is given in Table III.

Further Investigation of Intramolecular H-Bonding—Intramolecular H-bonding is among the most important interactions in biological molecules and is an internal cohesive force that can play an important role in determining the geometry and mode of recognition and association of biological molecules (27). In many instances, the presence of one or more H-bonds can be critical in determining the more stable conformer. Experimentally, the presence of H-bonding can be determined using solution NMR spectroscopy (28). NMR experiments designed to study intramolecular H-bonding generally rely on the premise that intramolecular H-bonding is less concentration-dependent than intermolecular H-bonding. In an intramolecular H-bond system, the proton participating in the hydrogen bond becomes more positive in its electronic character. As a consequence, this proton is deshielded compared with a non-hydrogen bonded proton, causing its signal to shift to a downfield in the NMR spectrum (28). This is usually the basis for measuring H-bonding using ^1H NMR.

To use this technique, the first step required identification of the two aliphatic OH resonances that were obscured by other resonances in the ^1H spectrum of CP-55,940 in $CDCl_3$ (Fig. 2), thus preventing a concentration dependence study. We approached this problem by obtaining the spectra in different solvents and with the use of two-dimensional exchange experiments. The two-dimensional exchange spectrum had two

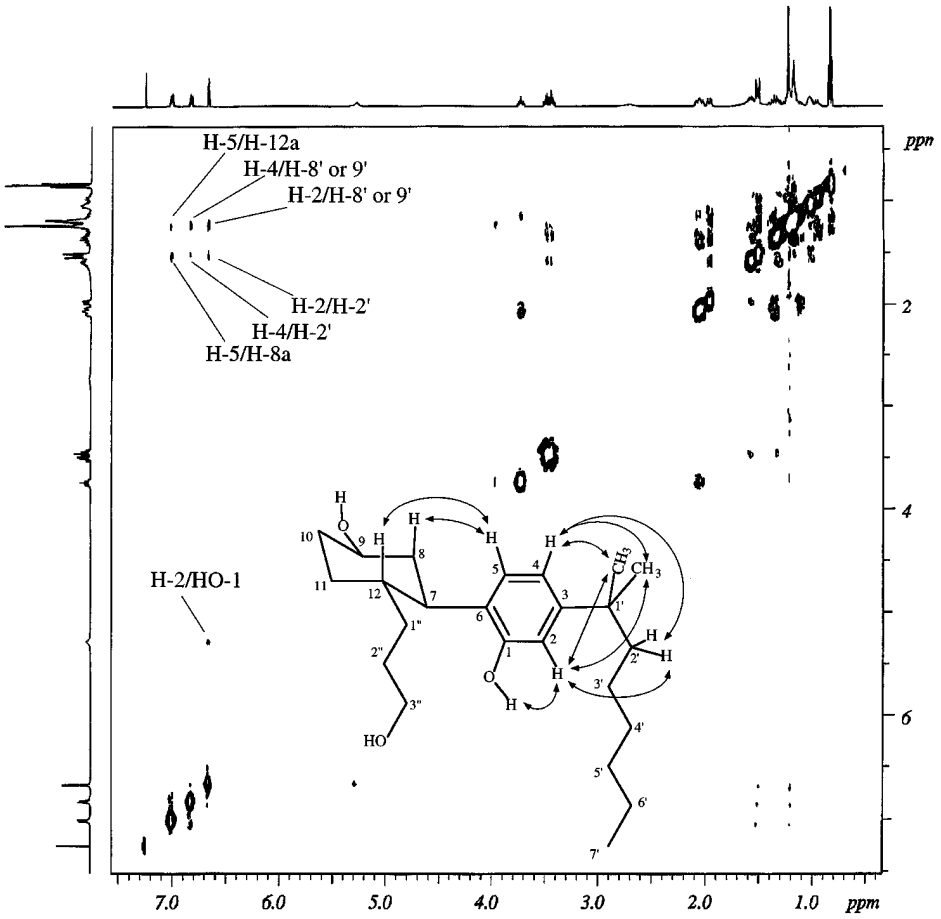

FIG. 5. **500 MHz NOESYPH spectrum in $CDCl_3$ at 298 K.** The NOE interactions for CP-55,940 are indicated with *arrows*.

strong positive cross-peaks generated through chemical exchange among the three OH groups and appearing at F1 = 1.55, F2 = 5.08 ppm and F1 = 1.24, F2 = 5.08 ppm, respectively. Differentiation of these two sets of positive cross-peaks could be accomplished by slicing out the cross-section plot of the two-dimensional exchange spectrum along the F2 dimension to obtain three positive peaks (Fig. 7). Of these, the most downfield positive peak at δ 5.08 ppm is due to the phenolic OH proton, whereas the most upfield situated peak centered at δ 1.24 ppm is due to the 3″-hydroxypropyl OH proton appearing as a triplet due to scalar coupling with the adjacent methylene protons (Fig. 7*A*). The peak at δ 1.55 ppm was readily assigned to the cyclohexyl 9-OH, whereas the peak at δ 1.64 ppm was shown to be due to an impurity in the commercial $CDCl_3$ solvent. The use of the two-dimensional ^1H-^1H exchange experiment thus allowed us to overcome the difficulty in identifying the two aliphatic OH peaks that overlapped with the methylene peaks in the one-dimensional spectrum.

Several two-dimensional exchange spectra were obtained using the same parameters while varying the concentration from 0.05 M to 0.0026 M. The one-dimensional cross-section due to the phenolic OH proton from each of the two-dimensional exchange spectra are shown in Fig. 7. This allows us to follow the effect of concentration on the ^1H chemical shifts of all three OH resonances. The results showed that the broad Ph-OH singlet at δ 5.08 ppm was the most concentration-dependent with a concentration coefficient of 10.8 ppm/mol; the 9-OH proton had a coefficient of 5.01 ppm/mol, whereas the 3″-OH triplet showed only a modest shift with a concentration coefficient of 2.3 ppm/mol. These results may be interpreted to mean that the 3″-OH proton is possibly engaged in intramolecular H-bonding with the phenolic OH and is thus less prone to chemical exchange or intermolecular H-bonding, whereas the phenolic OH hydrogen is more available for such interactions.

DISCUSSION

The combined use of two-dimensional NMR and computer molecular modeling has enabled us to define the conformational properties of CP-55,940 as discussed below.

Orientation of the Phenolic OH—The observed NOE cross-peak between the phenolic hydroxyl proton and the adjacent aromatic H-2 indicates that these two protons are spacially near each other and thus coupled through a dipole-dipole interaction (Fig. 5). Such a result implies that in its preferred conformation, the Ph-OH proton points away from the cyclohexyl ring and toward the H-2 proton. This result was also supported by our computational data showing that the phenolic O-H-bond lies in the plane of the aromatic ring and is oriented toward H-2. These findings are consistent with earlier results with the classical cannabinoid Δ^9-THC (19, 29, 35) and the nonclassical cannabinoid prototype CP-47,497 (13).

Orientation of the DMH Chain—The similar NOE cross-peak pattern observed as in the case of CP-47,497 (13) implies the possibility of several interconverting DMH side chain conformers that are time averaged on the NMR time scale. This conclusion was confirmed by our molecular modeling studies, which showed that the DMH side chain of CP-55,940 has an equal probability of existing in one of four minimum energy conformations, having a φ_3 dihedral angle of 60 °, −60 °, 120 °, and −120 °, respectively, and φ_4 equal to 60 ° and −60 °, respectively (Table III). In all the above conformations, the DMH side chain is almost perpendicular to the plane of the phenyl

ring. In these conformations, the 3′-CH_2 protons of the DMH side chain are located either above or below the plane of the aromatic ring. This conformational feature would account for the observed upfield shift (0.16 ppm *versus* 4′, 5′) of the 3′ protons, which can thus be attributed to the shielding effect of the phenyl ring.

Relative Orientation of the A- and C-rings—Two NOE cross-peaks were assigned to the spatial coupling of H-5 with H-8a and H-12a. Such cross-peaks are congruent with a calculated preferred conformation in which the planes of the two rings are almost perpendicular to each other and the Ph OH bond points down in the same plane as the axial H-7 and toward the α-face of the cyclohexyl ring (Fig. 5).

Additional information about the relative A/C-ring orientation was obtained from the NOESYVD spectrum (not shown) using a similar two-dimensional NOESYPH pulse sequence with four loops of randomly varied mixing times (800 ± 20 ms). In addition to the NOE cross-peak between H-5 with H-8a and H-12a, which was also observed in the previous NOESYPH spectrum, the spectrum had a very weak NOE cross-peak due to the interaction between the H-5 (δ 7.02 ppm) and H-7a (δ 2.72 ppm) protons. The presence of such an additional weak peak suggests the existence of two rotamers, a major one in which the phenolic OH is positioned toward the α-phase of the C-ring (φ_1 ~60 °) and a minor one in which the OH group faces up toward the β-face of the C-ring (φ_1 ~120°). The calculated relative energy difference between the above two conformations was found to be only 0.34 kcal/mol. The two rotamer populations interpreted on the basis of the extra NOE cross-peak is also congruent with the calculated high rotational energy barrier of CP-55,940 (20.5 kcal/mol), whereas the value for CP-47,497 is 9.7 kcal/mol, and no minor NOE between H-5 and H-7a was observed. Rotation about the C7-C6 bond on the NMR time scale was also indicated by a broad peak for H-7a with hardly discernible splitting in the one-dimensional ^{1}H NMR spectrum (Fig. 2) at room temperature. When the spectrum of CP-55,940 was obtained at a higher temperature (345 K), the peak for the H-7a resonance became a sharper and narrower triplet of triplets as in the case of CP-47,497, which indicates a faster rotational motion about the C7-C6 bond of CP-55,940 at a high temperature. Such an interpretation may also explain the apparent disappearance of the aromatic carbon C5 signal in the one-dimensional ^{13}C proton-decoupled broad band spectrum even when a delay as long as 120 s was used. Furthermore, the C5 carbon did not appear in the distortionless enhancement polarization transfer spectra and was not represented by a cross-peak in the hetero-COSY spectra. It was only with the help of a ^{1}H-^{13}C inverse detection HMQC spectrum, which is normally 10–100 times more sensitive than a conventional ^{13}C-detected hetero-COSY spectrum (17), that a cross-peak due to 5-CH could be observed. We attribute the low intensity of the C5 resonance in the ^{13}C spectrum to a broadening of this peak to the high rotational barrier around the C_6-C_7 bond. The detailed investigation will be published elsewhere.

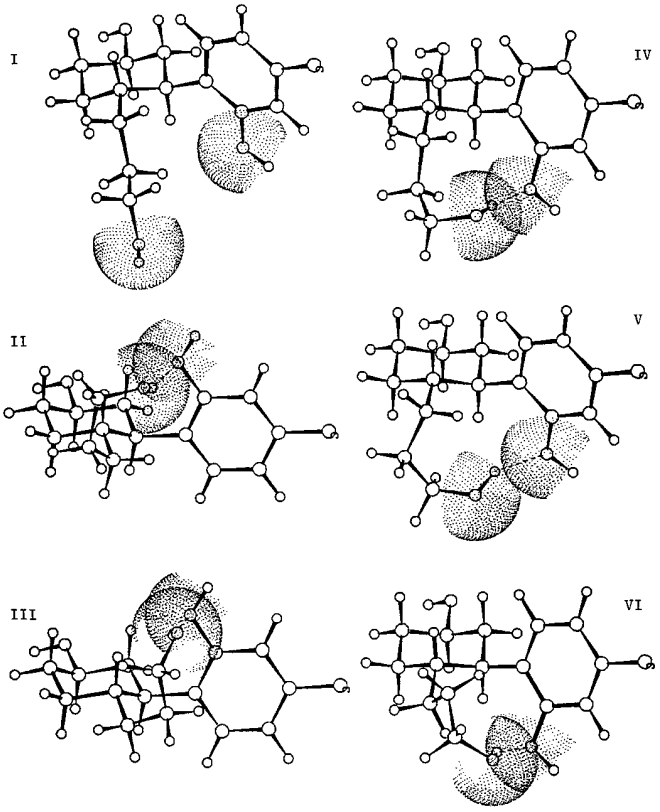

FIG. 6. **Molecular graphic representation of six energetically favored conformations of CP-55,940 on the basis of the energy minimization of structures occurring along the molecular dynamics trajectory.** The dimethylheptyl side chain is not displayed.

Conformation of the Southern Hydroxypropyl Chain—According to the one-dimensional and two-dimensional COSY ^{1}H spectra of CP-55,940, the 3″-CH_2 protons are nonequivalent. This is demonstrated by the features of the 3″-CH_2 multiples at δ 3.47 ppm in the one-dimensional spectrum (Fig. 2) and the presence of two cross-peaks due to coupling of each of the 3″-CH_2 protons with the vicinal 2″-CH_2. The above two spectra clearly show that the two 3″-CH_2 protons have different chemical shifts that differ by $\Delta\delta$ = 0.05 ppm. Theoretically, the two 3″-CH_2 protons should be equivalent because the low rotational energy barrier would allow the C2″-C3″ bond to rotate freely

TABLE III
Summary of structural features and relative energies of the conformations of CP-55,940 on the basis of the energy minimizations following dynamics simulations at 2500 K for 300 ps

No.	Time	Relative energy	Dihedral angles[a]		Intramolecular H-bonding[b]	
			(φ_1, φ_2, φ_3, φ_4)	(δ_1, δ_2, δ_3, δ_4)		
	ps	*kcal/mol*	*degrees*		*Å*	*degrees*
I	initial	0.11	(69, −0.3, −55, −55)	(−59, 178, −180, 180)	>4.0	
II	53	0.28	(−108, 4.5, 123, −56)	(168, −56, −47, 66)	2.11	157
III	81	2.86	(−118, 3, 121, −56)	(84, 63, −93, 44)	1.96	145
IV	177	0.00	(56, −8.9, 56, 56)	(−69, 160, −63, −39)	2.06	169
V	236	1.45	(70, −2, 56, 56)	(−89, 67, 56, −80)	2.01	143
VI	248	1.86	(48, −18, 55, 57)	(91, −165, 74, −42)	2.30	151
VII	261	0.78	(62, −0.7, −57, −55)	(180, −171, −179, 180)	>4.0	

[a] φ_1, φ_2, φ_3, and φ_4 are defined as the dihedral angles, C5-C6-C7-C8, C2-C1-O-H, C2-C3-C1′-C2′, and C3-C1′-C2′-C3′, respectively. δ_1, δ_2, δ_3, and δ_4 are defined as the dihedral angles, C7-C12-C1″-C2″, C12-C1″-C2″-C3″, C1″-C2″-C3″-O3″, and C2″-C3″-O3″-H3″.

[b] O3″-H—O1 Å represents the intramolecular H-bonding distances and angles between the proton of the hydroxypropyl 3″-OH (as a donor) and the oxygen of the phenolic hydroxyl group (as an acceptor).

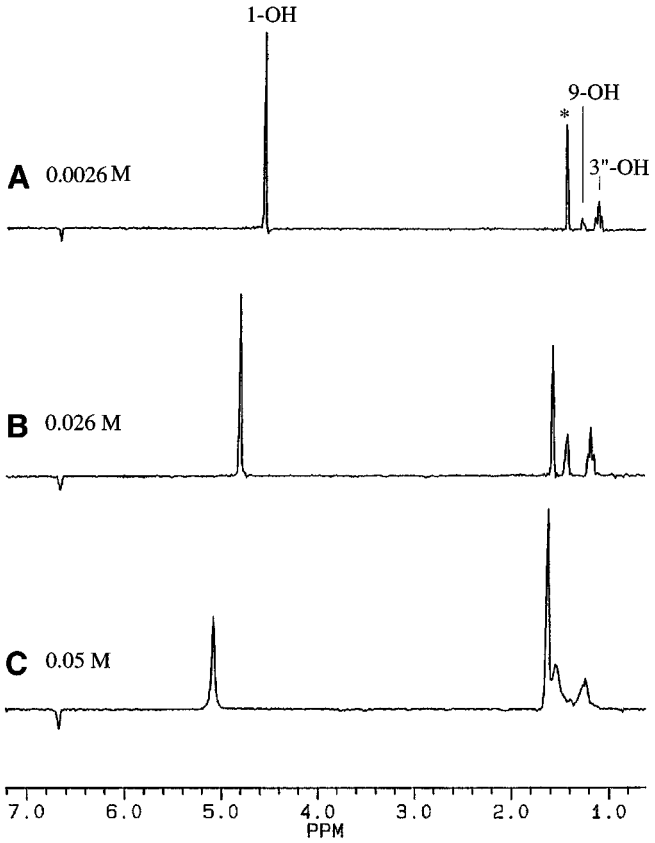

FIG. 7. **Cross-sections parallel to the F2 dimension sliced through the phenolic hydroxyl resonance in the 200 MHz two-dimensional ^{1}H chemical exchange spectrum of CP-55,940 in $CDCl_3$ at 298 K with the varied concentrations of 0.0026 (*A*), 0.026 (*B*), and 0.05 M (*C*).** The negative peak at δ 6.67 ppm is the NOE peak attributed to the dipolar coupling of H-2 with Ph-OH. The *asterisk* indicates the peak at 1.64 ppm that is due to an impurity from the $CDCl_3$ solvent).

and average out between the three rotamers. Therefore, the above observations imply some rotional restriction around the C2″–C3″ bond, possibly because of hydrogen bond formation between the 3″-OH and Ph-OH. Such a postulation is congruent with the earlier data regarding the spectroscopic properties of the three hydroxyl groups in CP-55,940.

The occurrence of an intramolecular H-bond was also supported by the result obtained from computer molecular modeling (Fig. 6). According to the combined experimental and theoretical data, the intramolecular H-bonding stabilizes the conformation of CP-55,940 by forming a ten-membered H-bonded ring. Based on these data, the most preferred conformation having an intramolecular H-bond was conformer IV in Fig. 8. Such a conformation is also congruent with the observed nonequivalency of the 3″-CH_2 protons because the ten-membered H-bonded ring would prevent free rotation in the hydroxypropyl chain. Our computational studies also revealed other conformers, especially conformer II in Fig. 8. Conformer II, differing from the IV by 0.28 kcal/mol, has all three hydroxyl groups pointing toward the same side of the molecule. Based on earlier (30, 31) studies from our laboratory, we postulate that a conformation such as II would be favored when these compounds partition into the cellular membrane because it would allow all three hydroxyls to interact with the polar side of the bilayer at the interface, whereas the other nonpolar parts of the molecule are associated with the hydrophobic bilayer chains. Such a conformer shares several stereochemical features of Δ^9-THC, whose preferred conformation is depicted in Fig. 8 (19, 22, 29, 35). As can be seen, the A- and C-rings of

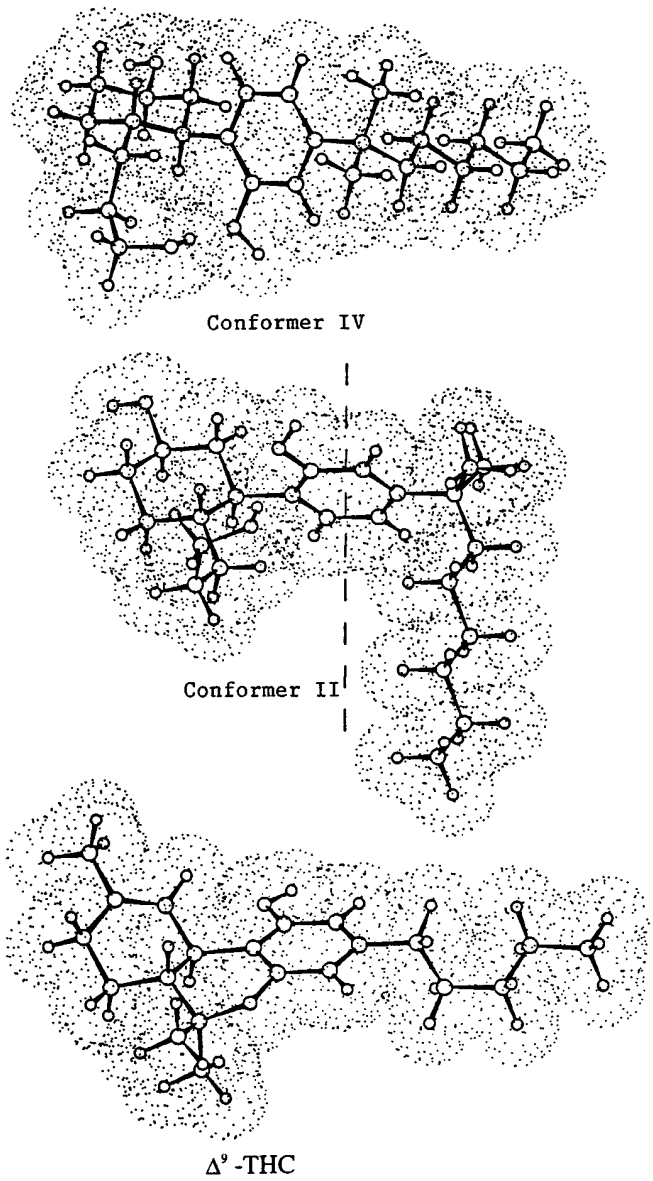

FIG. 8. **A graphical representation of the energetically most favored conformation of CP-55,940 stabilized by intramolecular H-bonding (IV), a low energy H-bonded conformer with all three OH groups pointing toward the one face of the molecule (II) and that of Δ^9-THC.** The conformation of Δ^9-THC was generated from the x-ray crystallographic data of Δ^9-tetrahydrocannabinolic acid (22) and energy-minimized using the Biosym program.

CP-55,940 can be superimposed on those of Δ^9-THC if the plane of its C-ring is rotated by 75 °, a process that requires an expenditure of 2~3 kcal/mol in energy as described elsewhere (13). The approximately 2 orders of magnitude higher potency of CP-55,940 when compared with Δ^9-THC can then be attributed to the additional structural features present in this molecule. They include a longer chain length, two α,α-dimethyl substituents in the side chain, the presence of a 9β-hydroxy, and a southern aliphatic hydroxypropyl group. All of these additional pharmacophores are expected to enhance the affinity of CP-55,940 for the cannabinoid receptor.

Conclusions—In this study, the high resolution NMR experiments provided detailed information on the conformation of CP-55,940 in solution and allowed us to identify a major preferred conformer as well as the presence of a minor rotamer. Molecular modeling studies confirmed that the preferred conformation in solution was indeed the low energy conformer but

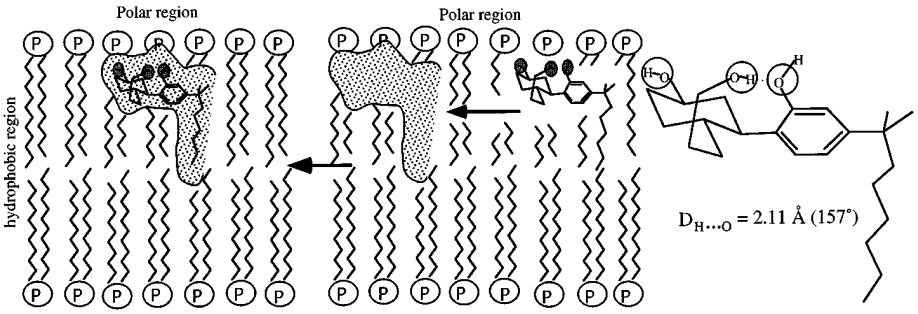

FIG. 9. **A ligand-membrane-receptor model representing the transmembrane diffusion of CP-55,940 en route to interacting with the cannabinoid receptor.** According to our hypothesis, the ligand preferentially partitions in the membrane bilayer where it assumes a proper orientation and location allowing for a productive collision with the active site.

also suggested at least one other low energy conformer that may be relevant to biological activity.

Our data show that the energetically favored conformations have the following features: (i) the A-ring is approximately perpendicular to the C-ring; (ii) the proton of Ph-OH points away from the C-ring; and (iii) the DMH chain randomly adopts one of four possible minimum energy conformations; however, in all cases, the DMH side chain is almost perpendicular to the plane of the phenyl ring. It is tempting to postulate that the dramatic increased potency of cannabinoid analogs with a 1′,1′-dimethylheptyl side chain when compared with those having no α-methyl substitution may be at least in part associated with the respective enforced conformational properties of the DMH side chain. Our results also show that the most energetically favored conformation for CP-55,940 is the one with Ph-OH pointing down toward the α-face of the C-ring. This conformation is stabilized through the formation of an intramolecular H-bond between the southern hydroxypropyl group and the Ph-OH as shown in Fig. 8 (IV). However, this energetically most favored conformer does not necessarily represent the preferred conformation at the active site. In this regard, our studies showed that another almost equienergetic conformer (II in Fig. 8), differing from IV by only 0.28 kcal/mol, may represent the pharmacophoric conformation. We might postulate that because of its amphipathic properties, CP-55,940 incorporates into biological membranes in its pharmacophoric conformation and assumes an orientation that allows all three hydroxyl groups to face the polar side of the bilayer, whereas in the bilayer, the cannabinoid ligand undergoes lateral diffusion and approaches the cannabinoid receptor in an orientation highly favorable for a productive collision with its binding site. This general hypothesis for the ligand-membrane-receptor systems has been discussed elsewhere (31, 32, 33) and is diagrammatically represented for CP-55,940 in Fig. 9. Currently, we are carrying out the further investigation of molecular dynamic and conformational properties for this ligand in a model membrane system.

Acknowledgment—We thank Dr. Susan S. Pochapsky for professional support.

REFERENCES

1. Dewey, W. L. (1986) *Pharmacol. Rev.* **38,** 151–178
2. Mechoulam, R. (ed) (1986) *Cannabinoids as Therapeutics Agents*, CRC Press, Inc., Boca Raton, FL
3. Howlett, A. C., Bidaut-Russell, M., Devane, W. A., Melvin, L. S., Johnson, M. R., and Herkenham, M. (1990) *Trends Neurosci.* **13,** 420–423
4. Bouaboula, M., Rinaldi, M., Carayon, P., Carillon, C., Delpech, B., Shire, D., Le Fur, G., and Casellas, P. (1993) *Eur. J. Biochem.* **214,** 173–180
5. Kaminski, N. E., Abood, M. E., Kessler, F. K., Martin, B. R., and Schatz, A. R. (1992) *Mol. Pharmacol.* **42,** 736–742
6. Munro, S., Thomas, K. L., and Abu-Shaar, M. (1993) *Nature* **365,** 61–65
7. Melvin, L. S., Johnson, M. R., Harbert, C. A., Milne, G. M., and Weissman, A. (1984) *J. Med. Chem.* **27,** 67–71
8. Johnson, M. R., and Melvin, L. S. (1986) in *Cannabinoids as Therapeutic Agents* (Mechoulam, R., ed.) pp. 121–146, CRC Press, Inc., Boca Raton, FL
9. Johnson, M. R., Melvin, L. S., Althuis, T. H., Bindra, J. S., Harbert, C. A., Milne, G. M., and Weissman, A. (1981) *J. Clin. Pharmacol.* **21,** (suppl.) 271–282
10. Howlett, A. C., Johnson, M. R., Melvin, L. S., and Milne, G. M. (1988) *Mol. Pharmacol.* **33,** 297–302
11. Howlett, A. C., Champion, T. M., Wilken, G. H., and Mechoulam, R. (1990) *Neuropharmacology* **29,** 161–165
12. Melvin, L. S., Milne, G. M., Johnson, M. R., Wilken, G. H., and Howlett, A. C. (1996) *Mol. Neuropharmacol.*, in press
13. Xie, X. Q., Yang, D. P., Melvin, L. S., and Makriyannis, A. (1994) *J. Med. Chem.* **37,** 1418–1426
14. Marion, D., and Wuthrich, K. (1983) *Biochem. Biophys. Res. Comm.* **113,** 967–974
15. Bodenhausen, G., Kogler, H., and Ernst, R. R. (1984) *J. Magn. Reson.* **58,** 370–388
16. Kessler, H., Oschkinat, H., and Loosli, H-R. (1987) in *Methods in Stereochemical Analysis* (Croasmun, W. R., and Carlson, R. M. K., eds.) Vol. 9, pp. 153–285, VCH Publishers, Inc., New York
17. Bax, A., and Subramanian, S. (1986) *J. Magn. Reson.* **67,** 565–569
18. Diehl, P., Kellerhals, H., and Lustig, E. (1972) in *NMR: Basic Principles and Progress* (Diehl, P., Fluck, E., and Kosfeld, R., eds.) pp. 1–96, Springer-Verlag New York Inc., New York
19. Kriwacki, R. W., and Makriyannis, A. (1989) *Mol. Pharmacol.* **35,** 495–503
20. Booth, H. (1969) *Prog. NMR Spectrosc.* **5,** 149–381
21. Biosym, InsightII/DISCOVER (version 2.0.0/2.7.0) Biosym Inc., San Diego, CA
22. Rosenqvist, E., and Ottersen, T. (1975) *Acta Chem. Scand.* **B29,** 379–384
23. Hagler, A. T., Osguthorpe, D. J., Dauber-Osguthorpe, P., and Hempel, J. (1985) *Science* **227,** 1309–1315
24. Weiner, S. J., Kollman, P. A., Case, D. A., Singh, U. C., Ghio, C., Algona, G., Profeta S., Jr., and Weiner, P. (1984) *J. Am. Chem. Soc.* **106,** 765–784
25. Rance, M., Sorensen, O. W., Bodenhausen, G., Wagner, G., Ernst, R. R., and Wuthrich, K. (1983) *Biochem. Biophys. Res. Comm.* **117,** 479–485
26. Fesik, S. W. (1989) in *Computer-Aided Drug Design, Methods and Applications* (Perun, T. J., and Propst, C. L., eds.) pp. 56–91, Marcel Dekker, Inc., New York
27. Jeffrey, G. A., and Saenger, W., eds. (1991) *Hydrogen Bonding in Biological Structures*, pp. 1–155, Springer-Verlag New York Inc., New York
28. Onda, M., Yamamoto, Y., Inoue, Y., and Chujo, R. (1988) *Bull. Chem. Soc. Jpn.* **16,** 4015–4021
29. Reggio, P. H., Greer, K. V., and Cox, S. M. (1989) *J. Med. Chem.* **32,** 1630–1635
30. Rhodes, D. G., Sarmiento, J. G., and Herbette, L. G. (1985) *Mol. Pharmacol.* **27,** 612–623
31. Makriyannis, A. (1995) in *Cannabinoid Receptors* (Pertwee, R., ed) Chapter 3, pp. 87–115, Academic Press, London
32. Makriyannis, A., and Rapaka, R. S. (1990) *Life Sci.* **47,** 2173–2184
33. Herbette, L. G. (1994) *Drug Dev. Res.* **33,** 214–224
34. Weiner, S. J., Kollman, P. A., Nguyen, D. T., and Case, D. A. (1986) *J. Comp. Chem.* **7,** 230–252
35. Reggio, P. H., and Mazurek, A. P. (1987) *J. Mol. Struct.* **149,** 331–343